

Nearly isentropic flow at sizeable η/s

Aleksi Kurkela^{1,2}, Urs Achim Wiedemann¹ and Bin Wu¹

¹ *Theoretical Physics Department, CERN, CH-1211 Genève 23, Switzerland*

² *Faculty of Science and Technology, University of Stavanger, 4036 Stavanger, Norway*

Abstract

Non-linearities in the harmonic spectra of hadron-nucleus and nucleus-nucleus collisions provide evidence for the dynamical response to azimuthal spatial eccentricities. Here, we demonstrate within the framework of transport theory that even the mildest interaction correction to a picture of free-streaming particle distributions, namely the inclusion of one perturbatively weak interaction (“one-hit dynamics”), will generically give rise to all observed linear and non-linear structures. We further argue that transport theory naturally accounts within the range of its validity for realistic signal sizes of the linear and non-linear response coefficients observed in azimuthal momentum anisotropies with a large mean free path of the order of the system size in peripheral ($\sim 50\%$ centrality) PbPb or central pPb collisions. As a non-vanishing mean free path is indicative of non-minimal dissipation, this challenges the perfect fluid paradigm of ultra-relativistic nucleus-nucleus and hadron-nucleus collisions.

Introduction. The applicability of relativistic transport theory ranges from the description of free-streaming particle distributions via weakly interacting systems of long mean free path up to systems exhibiting viscous fluid dynamic behavior. In this way, transport theory encompasses within a unified framework a broad range of candidate theories for the collective flow-like behavior observed in ultra-relativistic nucleus-nucleus [1] and, more recently, proton-nucleus [2, 3, 4], deuterium-nucleus [5, 6] and high multiplicity proton-proton collisions [7, 8].

Arguably the best-studied candidate theory for collective dynamics in nuclear collisions is the viscous fluid dynamic limit of kinetic transport. Fluid dynamic simulations of ultra-relativistic heavy ion collisions at RHIC and at the LHC can account for hadronic spectra in nucleus-nucleus collisions, their azimuthal anisotropies v_m , their p_T -differential hadrochemical composition, as well as for correlations between different v_m 's, see Refs. [9, 10] for recent reviews. Generically, these fluid dynamic simulations favor an almost perfect fluid with a very small ratio of shear viscosity to entropy density $\eta/s \sim \mathcal{O}(1/4\pi)$, suggesting that the system is so strongly interacting that the notion of quasi-particles and mean free path becomes doubtful since no particle excitation propagates over distances larger than $\mathcal{O}(1/T)$. However, up to finer differences [11, 12] that may or may not be improvable via tuning of model parameters, the main signal sizes and kinematic dependencies of v_m 's in nucleus-nucleus collisions have also been accounted for [13] by A-Multiphase-Transport-Model (AMPT) [14], a simulation code of partonic and hadronic transport whose applicability relies on a sufficiently large mean free path. The supposed dichotomy between a strong coupling picture (based on negligible mean free path and almost perfect fluidity) and a weak coupling picture based on spatially well-separated interactions is further challenged by the apparent phenomenologically compatibility of both descriptions with smaller collision systems. In particular, exploratory fluid dynamic simulations of pPb collisions have predicted [15, 16] for an almost perfect fluid ($\eta/s \sim (1-2)/4\pi$) the correct signal size and p_T -dependence of anisotropic elliptic and triangular flow in pPb prior to data taking at the LHC [2, 3, 4], while the AMPT code provides a phenomenologically reasonable description of pPb data at LHC [12] and smaller collision systems at RHIC [17] with an apparently dilute system from which approximately $\sim 50\%$ of all partons escape without rescattering [18] (numbers quoted for d+Au collisions at RHIC). The discovery of heavy ion like behavior in smaller (pp and pPb) collision systems at the LHC and its confirmation at RHIC energies thus raises the question of whether the matter produced in these collisions shares properties of an almost perfect fluid, or whether the observed signatures of collectivity can arise in a system of particle-like excitations of significant mean free path.

Increasing η/s in fluid dynamic simulations i) reduces the efficiency of translating spatial gradients into momentum

anisotropies and ii) increases entropy production. Within a model parameter space that includes uncertainties in the initial conditions, one may imagine to increase η/s by compensating effect i) with an increased initial density (and thus with increased initial spatial pressure gradients within a fixed initial spatial overlap area). But entropy increases with increasing initial density or η/s , and any such variation of model parameters is therefore tightly constrained by event multiplicity. This illustrates that a phenomenologically valid collective dynamics needs to combine a nearly isentropic dynamics with an efficient mechanism for translating spatial anisotropies into momentum anisotropies. Remarkably, in the opposite limiting cases of a (nearly) perfect liquid and of a (nearly) free-streaming gas of particles, kinetic transport theory gives rise to a (nearly) isentropic dynamics. The first limit is clearly realized in fluid dynamic simulations that are known to translate efficiently spatial into momentum anisotropies. At face value, the fact that transport codes like AMPT and MPC [19] can build up an efficient collective dynamics with very few spatially separated collisions indicates that they dynamically realize the opposite limit of a nearly isentropic evolution close to free-streaming. This has the potential for a shift away from the perfect fluid paradigm and it thus deserves to be understood in detail.

For any sufficiently complex simulation, the code *is* the model in the sense that the code is more than a tool for solving an easily stated set of equations of motion. For instance, fluid dynamic simulations do not code only for a solution to the viscous fluid dynamic equations of motion, but they interface those with a model of initial conditions, with a model for hadronization and with a hadronic rescattering phase. This necessary phenomenological complexity of a simulation can obscure the relation between phenomenological success and the physical mechanism at work. For state-of-the-art fluid dynamic codes, however, the fluid dynamic part of the simulation is benchmarked against analytically known results of viscous Israel-Stewart theory, and many kinematic dependencies and measurable properties of v_m 's and their correlations can be understood at least qualitatively by solving in isolation for the viscous fluid dynamic equations of motion with suitable initial conditions. It is the qualitative and semi-quantitative consistency between full phenomenological simulations and benchmarked solutions to an unambiguously defined set of equations of motion that gives strength to the phenomenological conclusion of fluid dynamic behavior in heavy ion collisions.

For transport theory close to the free streaming limit, a corresponding program of anchoring major dynamical stages of full-fledged simulations on unambiguously and analytically defined benchmark calculations is largely missing (exceptions include early tests of $2 \rightarrow 2$ parton cascades between the free-streaming and hydrodynamic limits [20, 21], more recent comparisons of kinetic theory to fluid dynamics [22, 23, 24]). What is at stake is to understand from simple physical principles and beyond any specific model implementation whether a particular manifestation of collective behavior is a *generic* property of transport theory. Motivated by the conceivable phenomenological relevance of transport close to the free-streaming limit for ultra-relativistic hadronic collision systems, the aim of this paper is to pursue such a programme of establishing benchmark results, and to determine which characteristic signatures of collectivity will arise generically in such a framework.

The model. We start from massless kinetic transport of a distribution $f(\vec{x}_\perp, \vec{p}, \tau)$, assuming longitudinal boost invariance and focussing on the slice of central spatial rapidity $\eta_s = 0$ [25],

$$\partial_\tau f + \vec{v}_\perp \cdot \partial_{\vec{x}_\perp} f - \frac{p^z}{\tau} \partial_{p^z} f = -C[f]. \quad (1)$$

We denote space-time coordinates by $\vec{x} = (x, y, z)$, $\vec{x}_\perp = (x, y)$ and normalized momenta by $v_\mu \equiv p_\mu/p$ with $p_\mu p^\mu = 0$ and $v^0 = 1$. We are mainly interested in p -integrated distribution functions $F(\vec{x}_\perp, \Omega, \tau) = \int \frac{4\pi p^2 dp}{(2\pi)^3} p f$ that satisfy

$$\partial_\tau F + \vec{v}_\perp \cdot \partial_{\vec{x}_\perp} F - \frac{1}{\tau} v_z (1 - v_z^2) \partial_{v_z} F + \frac{4v_z^2}{\tau} F = -C[F], \quad (2)$$

where Ω is the solid angle in the momentum space. In order to derive the above equation from eq. (1), we have taken f as a function of p, ϕ and v_z and we have used $\vec{v}_\perp = \sqrt{1 - v_z^2} (\cos \phi, \sin \phi)$. The collision kernel depends on the microscopic details of the interactions of the constituents. However, it is a generic property of interactions that they bring the system towards isotropy, and hence we consider a model — *isotropization-time approximation* — in which the scattering between particles in a given volume element is assumed to distribute the particles isotropically in the rest frame of that given volume element

$$-C[F] = -\gamma \varepsilon^{1/4}(x) [-v_\mu t^\mu] (F - F_{\text{iso}}), \quad (3)$$

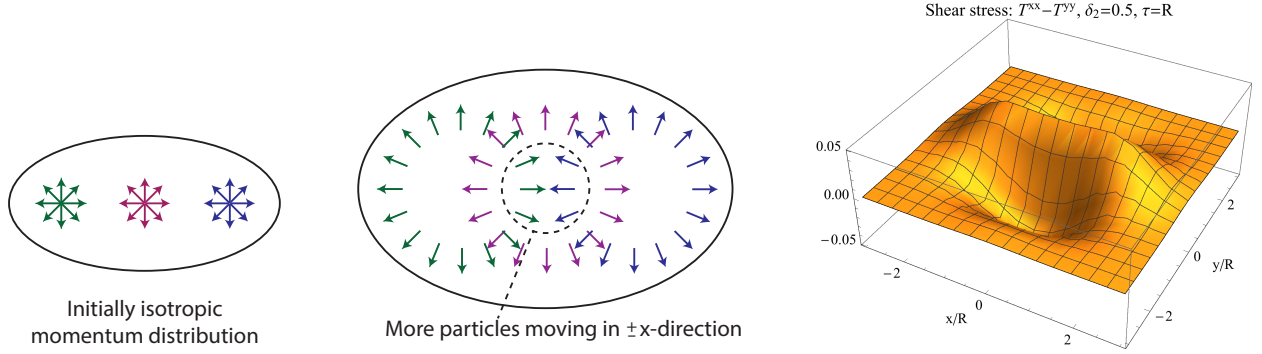


Figure 1: Combining transverse spatial eccentricity, free-streaming, and isotropizing scattering leads to global momentum space anisotropies: (Left) The system starts at τ_0 with an elliptic spatial eccentricity δ_2 . The particle production is local and hence momentum distributions at each point are isotropic. (Middle) Free-streaming particles move along the directions of their momentum vectors leading to *local* momentum anisotropies. In the central region where most collisions take place, there is an excess of particles moving horizontally compared to vertically moving ones. The interactions in the center region tend to isotropize the distribution function, and thus they reduce the number of horizontal movers and they add vertical movers. This generates a *global* momentum anisotropy. (Right) The local momentum space anisotropy measured by $T^{xx} - T^{yy}$ that results from free streaming an initial condition with eccentricity $\delta_2 = 0.5$ up to time $\tau = R$.

where F_{iso} is the isotropic distribution in the rest frame u^μ . We further assume that the system is conformally symmetric such that the time scale for the interactions is proportional to the energy density scale of the medium, $l_{\text{mfp}} \sim (\gamma \epsilon^{1/4})^{-1}$, where γ is our single model parameter setting the isotropization rate. While in more realistic models, different momentum scales isotropize on different timescales [26, 27], the momentum integral in the definition of F is dominated by a single scale, whose isotropization time corresponds to our model parameter (see e.g. [28] for a comparison of this model to QCD effective kinetic theory, finding $\sim 10\%$ differences in relaxation of $T^{\mu\nu}$ when η/s of the two models are matched). This caveat in mind, we shall restrain ourselves from making p_T -differential statements which would depend on details of the collision kernel that are not captured by a single isotropization timescale.

The local rest frame energy density ϵ and the rest frame velocity u_μ with normalization $u^\mu u_\mu = -1$ are defined by the Landau matching condition, $u^\mu T_\mu^\nu = -\epsilon u^\nu$, with the energy-momentum tensor defined by the second velocity moments of F . The form of F_{iso} can be found by demanding that the unintegrated isotropic distribution f_{iso} depends only on the Lorentz scalar $p^\mu u_\mu$, $f_{\text{iso}} = g(p^\mu u_\mu)$. Even though the exact functional dependence g is not known for a non-equilibrium system, the integrated isotropic distribution can be determined explicitly from the dimensionality of the integrand and the requirement $\int \frac{d^3 p}{(2\pi)^3} p^\mu u_\mu (f - f_{\text{iso}}) = 0$ of local energy conservation,

$$F_{\text{iso}}(\vec{x}_\perp, \Omega, \tau) = \int \frac{4\pi dp p^3}{(2\pi)^3} g(p u^\mu v_\mu) = \frac{\epsilon(\vec{x}_\perp, \tau)}{(-u_\mu v^\mu)^4}. \quad (4)$$

This isotropization time approximation is closely related to the usual relaxation time approximation, and in the hydrodynamical limit, its transport coefficients are $\tau_\pi = (\gamma \epsilon^{1/4})^{-1}$ and kinetic shear viscosity $\frac{\eta}{\epsilon+P} = \frac{\eta}{sT} = \frac{1}{\gamma \epsilon^{1/4}} \frac{1}{5}$. While kinetic theory (1) does not depend on the relation $\epsilon = aT^4$ between energy density and temperature, this relation enters if one wants to express the only model parameter γ in terms of the shear viscosity over entropy ratio. For $a \approx 13$ consistent with QCD lattice results, we find

$$\frac{\eta}{s} \approx \frac{0.11}{\gamma}. \quad (5)$$

Propagating eccentricities. We want to investigate how azimuthal anisotropies v_m in the transverse flow of energy density and non-linear correlations between these v_m 's arise in transport theory (2) for large mean free path l_{mfp} (i.e. small γ). Our starting point will be an azimuthally isotropic momentum distribution with vanishing longitudinal component $\propto \delta(v_z)$ distributed in a spatial profile that is longitudinally boost invariant and composed of an azimuthally isotropic background with perturbatively small deviations from azimuthal symmetry

$$F(\vec{x}_\perp, \phi, v_z, \tau = \tau_0) = 2\delta(v_z) \frac{(\epsilon_0 \tau_0)}{\tau_0} [F_0(\vec{x}_\perp, \phi, \tau = \tau_0) + \delta_2 F_{\delta_2}(\vec{x}_\perp, \phi, \tau = \tau_0) + \delta_3 F_{\delta_3}(\vec{x}_\perp, \phi, \tau = \tau_0) + \dots]. \quad (6)$$

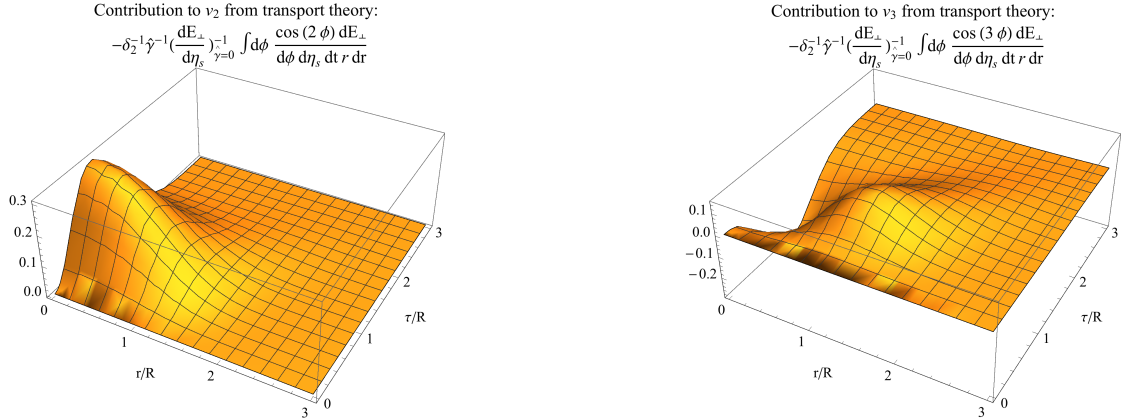


Figure 2: (Left) Contribution to v_2 arising from the $O(\delta_2)$ anisotropy as a function of time. The most of the signal is generated in the center region of the collision where the energy density is the highest at time $\tau \sim R$ when the momentum space anisotropy has developed but before the system has diluted due to radial expansion. (Right) Contribution to v_3 arising from the $O(\delta_3)$ anisotropy as a function of time.

The azimuthally symmetric initial background profile is of Gaussian form, $F_0(\vec{x}_\perp, \phi, \tau = \tau_0) = \exp[-(x^2 + y^2)/R^2]$ in the limit $\tau_0 \rightarrow 0$. The perturbations F_{δ_m} are *pure* in the m -th harmonic, $F_{\delta_2}(\vec{x}_\perp, \phi, \tau = \tau_0) = (r^2/R^2) \cos(2\theta) F_0(\vec{x}_\perp, \phi, \tau = \tau_0) = (x^2 - y^2) F_0(\vec{x}_\perp, \phi, \tau = \tau_0)/R^2$ in the limit $\tau_0 \rightarrow 0$ and similarly for the perturbation in $m = 3$ with $r^3 \cos(3\theta) = (x^3 - 3xy^2)$. Here, $\theta(\phi)$ denote the azimuthal angles in coordinate (momentum) space. Since the integration measure over the normalized longitudinal momentum $-1 < v_z < 1$ is $dv_z/2$, the factor 2 in front of (6) implies that $\varepsilon_0 = \varepsilon(\vec{x}_\perp = 0, \tau = \tau_0)$ is the initial energy density at the origin.

We want to determine how transport theory in the limit of large in-medium pathlength translates the small spatial perturbations δ_m into momentum anisotropies. To first order in $\gamma \propto 1/l_{\text{mfp}}$ (other analyses of this limit are found in Refs. [29, 30, 31, 32]), this amounts to a one-hit dynamics in which the initial distribution (6) is free-streamed up to proper time τ ,

$$F_{\text{free stream}}(x, y, \phi, \tau) = \frac{\tau_0}{\tau} F(x - (\tau - \tau_0) \cos \phi, y - (\tau - \tau_0) \sin \phi, \phi, \tau_0), \quad (7)$$

before entering once the collision kernel. The latter depends on F_{iso} , and thus it depends on the velocity u_μ of the local rest frame and on the comoving energy density ε . Both need to be determined from the free-streaming distribution (7). To this end, we make a tensor decomposition of

$$T^{\mu\nu} = \int \frac{d^3 p}{(2\pi)^3} \frac{p^\mu p^\nu}{p} f = \int_{-1}^1 \frac{dv_z}{2} \int \frac{d\phi}{2\pi} v^\mu v^\nu F. \quad (8)$$

For the azimuthally symmetric background distribution F_0 , the eigensystem of the resulting energy momentum tensor $T_0^{\mu\nu}$ can be given analytically in terms of the harmonic moments $A_m = \int \frac{d\phi}{4\pi} \cos(m\phi) \exp(-(\tau^2 + r^2 - 2\tau r \cos \phi)/R^2)$. In particular, $\varepsilon_0 = -(A_0 + A_2)/2 + A_1/u$ with $u = 4A_1 / \left(3A_0 + A_2 + \sqrt{9A_0^2 - 16A_1^2 + 6A_0A_2 + A_2^2} \right)$, and the background flow field is purely radial $u_\mu = (u_0 = \sqrt{1 - u_r^2}, u_r = u/\sqrt{1 - u^2}, u_\phi = 0, u_z = 0)$. Although free-streaming of F_0 preserves the global coordinate space azimuthal symmetry of the system, the presence of non-zero harmonics A_m in these expressions illustrates that local *momentum space anisotropies* develop over time. This is so, since the free-streaming distribution at any given position \vec{x}_\perp will depend on the direction ϕ in which particles propagate. Different positions have different anisotropies that the interactions tend to isotropize with the potential to create imbalance of the particle flow in the final state. In the azimuthally symmetric case the net effect is, however, zero and no anisotropy is generated. In contrast, in the case of an azimuthally anisotropic transverse profile momentum imbalance is generically formed as sketched in Fig. 1.

Small spatial eccentricities δ_m in the initial distribution (6) lead to computable perturbations of $T^{\mu\nu}$ away from $T_0^{\mu\nu}$. It is then straightforward to determine the eigensystem of the full energy momentum tensor perturbatively from that

of $T_0^{\mu\nu}$ to the needed order in the δ_m 's. For instance, the local energy density of the perturbed free-streaming solution is of the general form

$$\varepsilon = \varepsilon_0 + \sum_m \delta_m \tilde{\varepsilon}_m \cos(m\theta_m) + \sum_{m_1, m_2=1}^{\infty} \delta_{m_1} \delta_{m_2} \left(\sum_{\pm} \tilde{\varepsilon}_{m_1 m_2, m_1 \pm m_2} \cos(m_1 \theta_{m_1} \pm m_2 \theta_{m_2}) \right) + O(\delta_{m_i}^3), \quad (9)$$

where the tilde indicates that the angular dependence has been factored out. Here, $\theta_m \equiv \theta - \psi_m$ and equation (9) is written for a generalization of the initial conditions (6) for which different harmonic perturbations have different azimuthal reaction plane orientations ψ_m , that means $F_{\delta_m}(\vec{x}_{\perp}, \phi, \tau = \tau_0) = (r^m/R^m) \cos(m(\theta - \psi_m)) e^{-r^2/R^2}$. These coefficient functions $\tilde{\varepsilon}_*$ can be determined trivially in explicit form although they are generally lengthy. For instance

$$\tilde{\varepsilon}_2 = \frac{A_1(4r^2u + r\tau(3u^2 + 4) + 2\tau^2u)}{2R^2(u^2 - 1)} - \frac{A_2(r^2u^2 + 4r\tau u + \tau^2(u^2 + 2))}{2R^2(u^2 - 1)} + \frac{A_3\tau u(ru + 2\tau)}{2R^2(u^2 - 1)} + \frac{A_4\tau^2u^2/R^2}{4 - 4u^2} - \frac{A_0(2r^2(u^2 + 2) + 8r\tau u + \tau^2u^2)}{4R^2(u^2 - 1)}.$$

We have calculated analogously explicit but lengthy harmonic decompositions of the other eigenvalues and eigenvectors of the full perturbed energy momentum tensor $T^{\mu\nu} = T_0^{\mu\nu} + \delta T^{\mu\nu}$ that is obtained from free-streaming of (6). Armed with this information, we can determine the

Collision kernel and energy flow. Free-streaming leads to local azimuthal anisotropies of the spatial distribution, but the experimentally accessible momentum distribution remains azimuthally isotropic. To change the latter, collisions are needed to which we turn now. We are particularly interested in the measurable angular dependence of the radial flow of energy density at late time τ_{∞} when space-time rapidity η_s can be identified with momentum rapidity

$$2\pi \frac{dE_{\perp}}{d\eta_s d\phi} = \tau_{\infty} \int 2\pi d^2x_{\perp} \frac{dT^{0r}}{d\phi} = \tau_{\infty} \int d^2x_{\perp} \int \frac{2\pi p_{\perp} dp_{\perp}}{(2\pi)^2} \int \frac{dp_z}{(2\pi)} p_{\perp} f(\vec{x}_{\perp}, p_{\perp}, p_z, \phi, \tau_{\infty}). \quad (10)$$

Since $T^{\mu\nu}$ measures energy-momentum components per unit volume $d^2x_{\perp} dz$, the explicit τ_{∞} -dependence arises here from $dz = \tau_{\infty} d\eta_s$. After the last scattering at time τ' , the particles will free-stream from τ' to τ_{∞} . Since the \vec{x}_{\perp} -integration renders the free propagation trivial, $\int dp_z \int d^2x_{\perp} f(\vec{x}_{\perp}, p_{\perp}, p_z, \phi, \tau_{\infty}) = \frac{\tau'}{\tau_{\infty}} \int dp_z \int d^2x'_{\perp} f(\vec{x}'_{\perp}, p_{\perp}, p_z, \phi, \tau')$, we can undo this free-streaming and write eq. (10) as

$$2\pi \frac{dE_{\perp}}{d\eta_s d\phi} = \tau_{\infty} \int d^2x_{\perp} \int \frac{dv_z}{2} \sqrt{1 - v_z^2} F(\vec{x}_{\perp}, \phi, v_z, \tau_{\infty}) = \tau' \int d^2x_{\perp} \int \frac{dv_z}{2} \sqrt{1 - v_z^2} F(\vec{x}_{\perp}, \phi, v_z, \tau'). \quad (11)$$

Assuming only a single collision, the correction to the integrated distribution due to the interactions that take place in the infinitesimal time interval from τ' to $\tau' + d\tau'$ is given by $-C[F_{\text{free stream}}]d\tau'$. Then integrating over all possible times when the single interaction takes place, we get for the correction of order γ

$$2\pi \frac{dE_{\perp}}{d\eta_s d\phi} = \frac{dE_{\perp}}{d\eta_s} \Big|_{\gamma=0} - \int d\tau' \tau' \int d^2x_{\perp} \int \frac{dv_z}{2} \sqrt{1 - v_z^2} C[F_{\text{free stream}}](\vec{x}_{\perp}, \phi, v_z, \tau'). \quad (12)$$

The collision kernel that enters this one-hit dynamics is known explicitly from (2) and (4) in terms of the free-streamed solution $F_{\text{free stream}}$ obtained from the initial condition (6), the energy density ε calculated as described in (9) and the rest-frame velocity u_{μ} that we have also calculated perturbatively in powers of the eccentricities δ_m . Given that the δ_m -dependencies of $C[F_{\text{free stream}}]$ are known explicitly, we can Taylor expand in the eccentricities and perform the integrals in (11), thus obtaining the main result of this work

$$\begin{aligned} \frac{dE_{\perp}}{d\eta d\phi} = \frac{1}{2\pi} \frac{dE_{\perp}}{d\eta} \Big|_{\gamma=0, \delta_m=0} & \left\{ 1 - 0.210 \hat{\gamma} - 0.212 \hat{\gamma} \delta_2 2 \cos(2\phi - 2\psi_2) - 0.140 \hat{\gamma} \delta_3 2 \cos(3\phi - 3\psi_3) \right. \\ & + 0.063 \hat{\gamma} \delta_2^2 2 \cos(4\phi - 4\psi_2) + 0.015 \hat{\gamma} \delta_2^2 + 0.112 \hat{\gamma} \delta_3^2 2 \cos(6\phi - 6\psi_3) + 0.043 \hat{\gamma} \delta_3^2 \\ & \left. + 0.088 \hat{\gamma} \delta_2 \delta_3 2 \cos(5\phi - 3\psi_3 - 2\psi_2) \right\}, \end{aligned} \quad (13)$$

where we have followed the angular dependence analytically and performed the remaining r - and τ -integrals numerically.

Dimensional analysis of the kinetic theory (2) reveals that irrespective of the initial conditions, physical results like (13) depend only on one particular combination of system size R , initial energy density ε_0 and scale γ of the inverse mean free path.

$$\hat{\gamma} = R^{3/4} \gamma (\varepsilon_0 \tau_0)^{1/4} \approx R \gamma (e \varepsilon(\vec{x}_\perp = 0, \tau = R))^{1/4} \approx 1.28 R \gamma \varepsilon^{1/4}(\vec{x}_\perp = 0, \tau = R). \quad (14)$$

Here, the latter form shows that the expansion parameter is proportional to the mean free path at time $\tau = R$ when flow is mainly generated; it is obtained with the help of $\varepsilon(\vec{x}_\perp = 0, \tau) = \tau_0 \varepsilon_0 e^{-\tau^2/R^2} / \tau + \mathcal{O}(\gamma, \delta)$. The one-hit dynamics studied here is a truncation of transport theory to first order in $\hat{\gamma} \sim R/l_{\text{mfp}}$. This expansion is justified for $\hat{\gamma} < \mathcal{O}(1)$ but it breaks down for $\hat{\gamma} > \mathcal{O}(1)$. This is clearly seen from the correction to free-streaming for an azimuthally symmetric distribution (the term $\propto -0.210\hat{\gamma}$) that renders (13) unphysical for $\hat{\gamma} > 1/0.210$. This term arises from scatterings that transfer transverse into longitudinal momentum and it indicates that multiple scatterings need to be resummed for $\hat{\gamma}$ of this order.

Within its range of validity ($\hat{\gamma} < \mathcal{O}(1)$), the main qualitative conclusion of (13) is that both, linear response to spatial eccentricities and non-linear mode-mode coupling are natural consequences of a perturbative one-hit dynamics and thus must not be taken for a tell-tale sign of a hydrodynamic mechanism at work. In fact, we could have easily expanded (13) to higher orders in eccentricities to obtain higher non-linear mode-mode couplings (such as $v_6 \propto \delta_2^3$) or we could have included higher harmonics in the initial condition (6) to find e.g. linear response coefficients v_4/δ_4 and v_5/δ_5 . All the linear and non-linear structures observed in the azimuthal distributions of single inclusive hadron spectra can be obtained from transport models in the limit of long mean free path.

A quantitative comparison of the coefficients in (13) to other model calculations and data is complicated by several issues. For instance, v_m coefficients are typically defined as azimuthal anisotropies of particle distributions $\frac{dN}{p_\perp dp_\perp d\eta d\phi}$. Instead, eq. (13) provides anisotropies $\frac{dE_\perp}{d\eta d\phi} \propto \frac{dE_\perp}{d\eta} [1 + 2 \sum_{m=1} v_m \cos(m\phi - m\psi_m)]$ of the p_T -integrated transverse energy flow. Due to the different p_\perp -weighting, $dE_\perp = p_\perp dN$, the anisotropies thus obtained can be $\mathcal{O}(30\%)$ larger. Also, the prefactors in (13) are model-dependent in the sense that they depend on the shape of the transverse profile of the initial condition. Only to the extent to which the dynamical response to main spatial characteristics such as δ_2 and δ_3 is robust against finer details of transverse profile, can the response coefficients calculated here be taken as indicative of the typical signal sizes obtained from transport theory in the one-hit limit. We note in this context that constructions of linear response coefficients by dividing data on v_m with values of δ_m obtained from model calculations [1, 33] show variations of $\mathcal{O}(30\%)$ depending on the model from which the eccentricities are calculated. While these considerations caution us that any numerical comparison at face value can only be indicative of order of magnitude effects, we nevertheless share in the following numerical observations to address the fundamental question whether a transport mechanism with significant mean free path can be sufficiently efficient to account for the observed signal size within the range of its validity.

We base the following numerical comparison on one particularly compact and recent compilation of linear and non-linear response coefficients, see Fig. 1 of Ref. [33]. This study shows values for v_2/δ_2 (v_3/δ_3) that drop from ~ 0.3 (~ 0.2) in the most central (0-5%) PbPb collisions at 2.76 TeV to values ~ 0.1 in the most peripheral 70-80% (in peripheral 40-50% centrality) collisions. At face value, if we assume $\hat{\gamma} \sim 1$ in peripheral PbPb collisions of $\sim 50\%$ centrality, then these findings are consistent with the numbers extracted from (13) to leading order in $\hat{\gamma}$

$$\frac{v_2}{\delta_2} = 0.212\hat{\gamma}, \quad \frac{v_3}{\delta_3} = 0.140\hat{\gamma}. \quad (15)$$

We note that the factor $(1 - 0.210\hat{\gamma})$ of the zeroth harmonic in (13) would enter (15) only to higher order in $\hat{\gamma}$, where our calculation is not complete. In analogy to (15), one can construct linear response coefficients for central pPb collisions at 5.02 TeV by dividing the measured v_m asymmetries ($v_2 \sim 0.06$, $v_3 \sim 0.02$ [34]) by estimates of average eccentricities in hadron-nucleus collisions ($0.25 < \delta_2 < 0.34$, $0.18 < \delta_3 < 0.32$, [16]). Again, this lies in the ballpark of (15) for $\hat{\gamma} \sim 1$. Within the above-mentioned uncertainties, this indicates that the range of validity of one-hit dynamics extends to systems as large as those created in peripheral PbPb ($\sim 50\%$ centrality) or central pPb collisions.

For a choice $\hat{\gamma} \sim 1$, also the size of the major non-linear mode-mode couplings extracted from (13)

$$\frac{v_4}{\delta_2^2} = 0.063\hat{\gamma}, \quad \frac{v_5}{\delta_2 \delta_3} = 0.088\hat{\gamma}, \quad (16)$$

seem to be, within the stated uncertainties, consistent with the strength of the couplings in peripheral ($\sim 50\%$ centrality) PbPb collision shown in Ref. [33], thus reinforcing the qualitative conclusion drawn from the comparison to linear response coefficients. However, the contribution to v_6 in (13) seems to be significantly larger than the value shown in Ref. [33]. We note in this context that while the coefficients in (15) and (16) are generated within a time $\tau \sim R$ comparable to the system size (see Fig. 2), significant contributions to v_6 come in our calculation from times as late as $\tau \sim 4R$. We refrain from speculating whether these or other reasons are at the origin of the observed discrepancy for $v_6/\delta_3 \delta_3$.

Further qualitative and quantitative features of measured momentum anisotropies may also be consistent with one-hit dynamics. For instance, it has been argued in [31] that the experimentally observed mass ordering of v_n 's can also result as a generic feature of one-hit dynamics. This is so, because the dynamics leading to v_n 's depends essentially on velocities, and this corresponds to a mass ordering in the transverse momenta.

Since the mean free path l_{mfp} at the typical time $\tau = R$ at which scattering occurs in our calculation is $l_{\text{mfp}} = \gamma^{-1} \varepsilon^{-1/4}(\vec{x}_\perp = 0, \tau = R)$, it follows from (14) that $\hat{\gamma} \sim 1$ corresponds to $N_{\text{coll}} \sim 1$ collision per particle per system size. Since $l_{\text{mfp}} = \gamma^{-1} \varepsilon^{-1/4}(\vec{x}_\perp = 0, \tau = R)$ remains almost unchanged with system size while $\hat{\gamma}$ increases almost linearly with system size, the same transport theory that accounts with $\hat{\gamma} \sim 1$ for peripheral PbPb collisions would automatically apply to more central nucleus-nucleus collisions. It is not the transport theory, but only its one-hit approximation studied here that becomes more questionable for increasing centrality; the intrinsic matter properties of the system remain (almost) unchanged with centrality.

It may be noteworthy that also the AMPT (see Figs. 1 and 2 of Ref. [18]) and BAMPS [35] transport codes simulate central hadron-nucleus collisions with $N_{\text{coll}} \sim 1$ collision. Of course, the number N_{coll} or the mean free path is not free of model-dependent assumptions about the nature of the collision. In the transport theory (1), the mean free path l_{mfp} corresponds to the time scale over which a distribution F evolves to the isotropic one F_{iso} . If instead a more sophisticated collision kernel dominated by small-angle scatterings is implemented in a transport code, a larger number of collisions may be needed for isotropization. Thus, in any given transport code, the efficiency to isotropize will depend on the microscopic dynamics (whose specification introduces some model-dependence); and in the present transport theory (1), this isotropization efficiency is parametrized in terms of one single parameter γ , irrespective of how it arises microscopically. There is no reason that eq. (1) must arrive at the same number of collisions than a transport code (that may supplement transport mechanisms by other model-dependent features such as string melting, hadronization prescriptions, etc), but the study of (1) teaches us that there is a class of transport models that can generate within the range of their validity a distribution (13) by a microscopic dynamics that realizes a particular value of γ .

For transport theory to apply, the mean free path of quasi-particles must be larger than the typical size of their wave-packets [39], $l_{\text{mfp}} > 1/T$. Here, we have argued that $\hat{\gamma} \sim 1$ describes peripheral (50% centrality) PbPb collisions which corresponds to a mean free path of the order of the transverse size of these collisions and which is significantly larger than the expected inter-particle distance $\sim 1/T$ in PbPb collisions. This supports the applicability of transport theory to ultra-relativistic pA and AA collisions. Indeed, the relation $l_{\text{mfp}} = 5 \frac{\eta}{sT} > 1/T$ suggests that transport theory may be applicable to systems of small shear viscosity over entropy ratio, as long as $\eta/s \gtrsim 0.2$. To extract the shear viscosity over entropy density ratio η/s for 50% central PbPb collisions described by $\hat{\gamma} \sim 1$, we use that the transverse energy produced in such collisions is set by measured quantities, $\frac{dE_\perp}{d\eta} = \langle p_\perp \rangle \langle \frac{dN}{d\eta} \rangle \approx 100 \text{ GeV}$ [37] and their system size R can be estimated from the nuclear overlap function at impact parameter $\sim 10 \text{ fm}$ [38], which is $R \sim 3 \text{ fm}$. In our set-up, $\frac{dE_\perp}{d\eta} = \pi R^3 e \varepsilon(R)$ converts these values to an energy density at time $\tau = R$ that takes the value $\varepsilon(R) \approx (240 \text{ MeV})^4$. This leads to $\frac{1}{\gamma} = e^{1/4} R \varepsilon^{1/4}(R) \approx 4.6$ and, given that the above estimates were taken on the conservative side, this translates according to eq. (5) into a shear viscosity

$$\eta/s = \frac{0.11}{\hat{\gamma}} \left(\frac{R dE_\perp}{\pi d\eta} \right)^{1/4} \approx 0.5 \quad (17)$$

or larger. Uncertainties about the centrality class for which $\hat{\gamma} \sim 1$ enter this expression only via the fourth root of the system size and the transverse energy in that centrality class. This makes the above estimate robust. We recall that for a kinetic transport description, η/s is a derived quantity that requires specifying the relation between energy density and temperature which does not enter the dynamical evolution. In the BAMPS transport model with parameter settings that reproduce data from nucleus-nucleus collisions at RHIC and at the LHC, a corresponding (somewhat

temperature-dependent) value for η/s was obtained [36] that in the low temperature range in which flow is built up is indeed roughly consistent with the estimate (17). We are unaware of other transport model comparisons to data that quote values of η/s . We note that the estimate (17) is a factor 6 larger than the perfect fluid limit $\eta/s = 1/4\pi$. Also, remarkably, evaluating the perturbative QCD result [40, 41, 42] with realistic values for the QCD coupling constant results in a value for η/s of similar magnitude. While the value of η/s supported by the present study is still exceptionally small compared to that of common substances like helium, nitrogen or water [43], it suggests that the systems created in nucleus-nucleus and proton-nucleus collisions may differ from the perfect fluid paradigm in that they allow for quasi-particles of significant mean free path.

We acknowledge helpful discussions with Ulrich Heinz.

References

- [1] K. Aamodt *et al.* [ALICE Collaboration], Phys. Rev. Lett. **107** (2011) 032301 [arXiv:1105.3865 [nucl-ex]].
- [2] B. B. Abelev *et al.* [ALICE Collaboration], Phys. Rev. C **90** (2014) no.5, 054901 [arXiv:1406.2474 [nucl-ex]].
- [3] V. Khachatryan *et al.* [CMS Collaboration], Phys. Rev. Lett. **115** (2015) no.1, 012301 [arXiv:1502.05382 [nucl-ex]].
- [4] M. Aaboud *et al.* [ATLAS Collaboration], Eur. Phys. J. C **77** (2017) no.6, 428 [arXiv:1705.04176 [hep-ex]].
- [5] A. Adare *et al.* [PHENIX Collaboration], Phys. Rev. Lett. **114** (2015) no.19, 192301 [arXiv:1404.7461 [nucl-ex]].
- [6] L. Adamczyk *et al.* [STAR Collaboration], Phys. Lett. B **747** (2015) 265 [arXiv:1502.07652 [nucl-ex]].
- [7] V. Khachatryan *et al.* [CMS Collaboration], Phys. Lett. B **765** (2017) 193 [arXiv:1606.06198 [nucl-ex]].
- [8] G. Aad *et al.* [ATLAS Collaboration], Phys. Rev. Lett. **116** (2016) no.17, 172301 [arXiv:1509.04776 [hep-ex]].
- [9] U. Heinz and R. Snellings, Ann. Rev. Nucl. Part. Sci. **63** (2013) 123 [arXiv:1301.2826 [nucl-th]].
- [10] P. Romatschke and U. Romatschke, arXiv:1712.05815 [nucl-th].
- [11] J. Adam *et al.* [ALICE Collaboration], Phys. Lett. B **753** (2016) 126 [arXiv:1506.08032 [nucl-ex]].
- [12] A. Bzdak and G. L. Ma, Phys. Rev. Lett. **113** (2014) no.25, 252301 [arXiv:1406.2804 [hep-ph]].
- [13] J. Xu and C. M. Ko, Phys. Rev. C **84** (2011) 044907 [arXiv:1108.0717 [nucl-th]].
- [14] Z. W. Lin, C. M. Ko, B. A. Li, B. Zhang and S. Pal, Phys. Rev. C **72** (2005) 064901 [nucl-th/0411110].
- [15] P. Bozek, Phys. Rev. C **85** (2012) 014911 [arXiv:1112.0915 [hep-ph]].
- [16] P. Bozek and W. Broniowski, Phys. Rev. C **88** (2013) no.1, 014903 [arXiv:1304.3044 [nucl-th]].
- [17] J. D. Orjuela Koop, A. Adare, D. McGlinchey and J. L. Nagle, Phys. Rev. C **92** (2015) no.5, 054903 [arXiv:1501.06880 [nucl-ex]].
- [18] L. He, T. Edmonds, Z. W. Lin, F. Liu, D. Molnar and F. Wang, Phys. Lett. B **753** (2016) 506 [arXiv:1502.05572 [nucl-th]].
- [19] D. Molnar and M. Gyulassy, Phys. Rev. C **62** (2000) 054907 doi:10.1103/PhysRevC.62.054907 [nucl-th/0005051].
- [20] M. Gyulassy, Y. Pang and B. Zhang, Nucl. Phys. A **626** (1997) 999 doi:10.1016/S0375-9474(97)00604-0 [nucl-th/9709025].
- [21] B. Zhang, M. Gyulassy and Y. Pang, Phys. Rev. C **58** (1998) 1175 doi:10.1103/PhysRevC.58.1175 [nucl-th/9801037].
- [22] A. Gabbana, M. Mendoza, S. Succi and R. Tripiccion, Phys. Rev. E **96** (2017) no.2, 023305 [arXiv:1704.02523 [physics.comp-ph]].
- [23] I. Bouras, E. Molnar, H. Niemi, Z. Xu, A. El, O. Fochler, C. Greiner and D. H. Rischke, Phys. Rev. C **82** (2010) 024910 [arXiv:1006.0387 [hep-ph]].
- [24] A. Kurkela and Y. Zhu, Phys. Rev. Lett. **115** (2015) no.18, 182301 [arXiv:1506.06647 [hep-ph]].
- [25] G. Baym, Phys. Lett. **138B**, 18 (1984).
- [26] P. B. Arnold, G. D. Moore and L. G. Yaffe, JHEP **0301** (2003) 030 doi:10.1088/1126-6708/2003/01/030 [hep-ph/0209353].
- [27] A. Kurkela and U. A. Wiedemann, arXiv:1712.04376 [hep-ph].
- [28] M. P. Heller, A. Kurkela and M. Spalinski, arXiv:1609.04803 [nucl-th].
- [29] H. Heiselberg and A. M. Levy, Phys. Rev. C **59** (1999) 2716 doi:10.1103/PhysRevC.59.2716 [nucl-th/9812034].
- [30] P. F. Kolb, P. Huovinen, U. W. Heinz and H. Heiselberg, Phys. Lett. B **500** (2001) 232 doi:10.1016/S0370-2693(01)00079-X [hep-ph/0012137].
- [31] N. Borghini and C. Gombeaud, Eur. Phys. J. C **71** (2011) 1612 doi:10.1140/epjc/s10052-011-1612-7 [arXiv:1012.0899 [nucl-th]].
- [32] P. Romatschke, arXiv:1802.06804 [nucl-th].
- [33] P. Liu and R. A. Lacey, arXiv:1802.06595 [nucl-ex].
- [34] A. M. Sirunyan *et al.* [CMS Collaboration], arXiv:1710.07864 [nucl-ex].
- [35] M. Greif, C. Greiner, B. Schenke, S. Schlichting and Z. Xu, Phys. Rev. D **96** (2017) no.9, 091504 [arXiv:1708.02076 [hep-ph]].
- [36] J. Uphoff, F. Senzel, O. Fochler, C. Wesp, Z. Xu and C. Greiner, Phys. Rev. Lett. **114** (2015) no.11, 112301 [arXiv:1401.1364 [hep-ph]].
- [37] K. Aamodt *et al.* [ALICE Collaboration], Phys. Rev. Lett. **106** (2011) 032301 [arXiv:1012.1657 [nucl-ex]].
- [38] P. F. Kolb, U. W. Heinz, P. Huovinen, K. J. Eskola and K. Tuominen, Nucl. Phys. A **696** (2001) 197 [hep-ph/0103234].
- [39] P. Danielewicz and M. Gyulassy, Phys. Rev. D **31** (1985) 53.
- [40] P. B. Arnold, G. D. Moore and L. G. Yaffe, JHEP **0011** (2000) 001 [hep-ph/0010177].
- [41] P. B. Arnold, G. D. Moore and L. G. Yaffe, JHEP **0305** (2003) 051 [hep-ph/0302165].
- [42] J. Ghiglieri, G. D. Moore and D. Teaney, arXiv:1802.09535 [hep-ph].
- [43] P. Kovtun, D. T. Son and A. O. Starinets, Phys. Rev. Lett. **94** (2005) 111601 doi:10.1103/PhysRevLett.94.111601 [hep-th/0405231].